

## Adsorption Removal of Humic Acid from Water Using a Modified Algerian Bentonite

S. Bousba<sup>a,\*</sup>, N. Bougdah<sup>b</sup>, N. Messikh<sup>b</sup> and P. Magri<sup>c</sup>

<sup>a</sup>*Département de Génie des Procédés, Faculté de Génie des Procédés, Université Salah Boubnider Constantine 3, Algérie.*

<sup>b</sup>*Département de Pétrochimie et Génie des Procédés, Faculté de Technologie, Université 20 Août 1955-Skikda, Algérie.*

<sup>c</sup>*LCP-A2MC, Université de Lorraine, 1, bd Arago-57078 METZ, Cedex 3, France*

*(Received 1 May 2018, Accepted 14 June 2018)*

In this study, the main objective is the preparation and the characterization of a modified Algerian bentonite based adsorbent by intercalation with hexadecyltrimethylammonium bromide (HDTMA). Natural and modified bentonites were characterized using thermogravimetric analysis (TGA), X-ray diffraction (XRD) and infrared spectroscopy (FTIR). The X-ray results indicated that the geometry of the interlayer space changes by the intercalation of HDTMA cations, resulting in an increase in the basal spacing from 1.34 to 1.96 nm. The adsorption efficiency of natural and HDTMA-bentonite was examined for humic acid (HA) removal by batch adsorption experiments under different operating conditions. The maximum monolayer adsorption capacity  $q_m$  of HA was found to be 54.80 mg g<sup>-1</sup> and 330.34 mg g<sup>-1</sup> for natural and HDTMA-bentonite, respectively. The kinetic study indicated that HA adsorption followed the pseudo-first-order model. Both natural and HDTMA-bentonite showed quite good capabilities in removing HA from aqueous solutions.

**Keywords:** Adsorption, Bentonite, HDTMA, Intercalation, Humic acid

### INTRODUCTION

Humic acid (HA) is a subclass of humic substances (HS) representing a component of natural organic matter (NOM) due to biological decomposition of organic matter from plants and other organisms. HS are mainly composed of HA, fulvic acid and humin, and are principally present in soil, geological organic deposits and water [1]. The model structure of HA as proposed by Stevenson [2] is shown in Fig. 1. The presence of HA in natural waters causes various environmental and health problems, such as undesirable color and taste of water [3]. Conventional drinking water treatment methods such as chlorination involve the production of disinfection by-products (DBPs), such as trihalomethanes (THMs) and haloacetic acids (HAAs), which are believed to be two harmful compounds to human health. Therefore, the elimination of HA from

drinking water is of significant importance before the addition of chlorine.

Treatment of water containing HA has been studied by various techniques such as membrane filtration [4], coagulation [5], advanced oxidation [6] and adsorption [7]. The adsorption technique is a wastewater treatment processes commonly used for the removal of low concentrations organic pollutants [8]. In recent years, there has been a growing interest in developing new bentonite-based adsorbents able to effectively remove organic and inorganic pollutants from water [9]. Bentonite clay is a very abundant and low-cost material in Algeria, the annual production of natural bentonite reach 27, 668 metric tons in 2013 [10].

In this context, this study aims to test the ability of natural and modified Algerian bentonite clays to adsorb HA from water. The Algerian bentonite was modified with the cationic surfactants hexadecyltrimethylammonium bromide C<sub>19</sub>H<sub>42</sub>NBr (HDTMA) to try to increase its adsorption

\*Corresponding author. E-mail: bousba\_salim@yahoo.fr

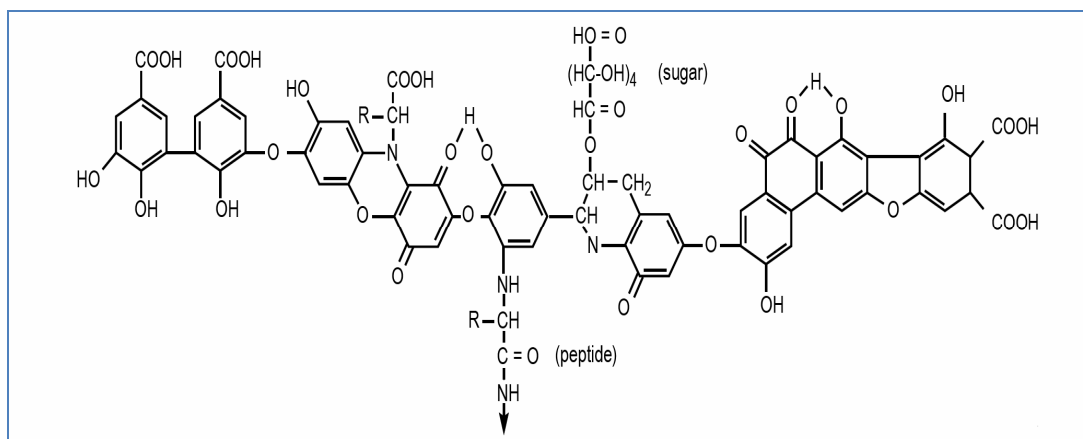


**Fig. 1.** Model structure of humic acid.

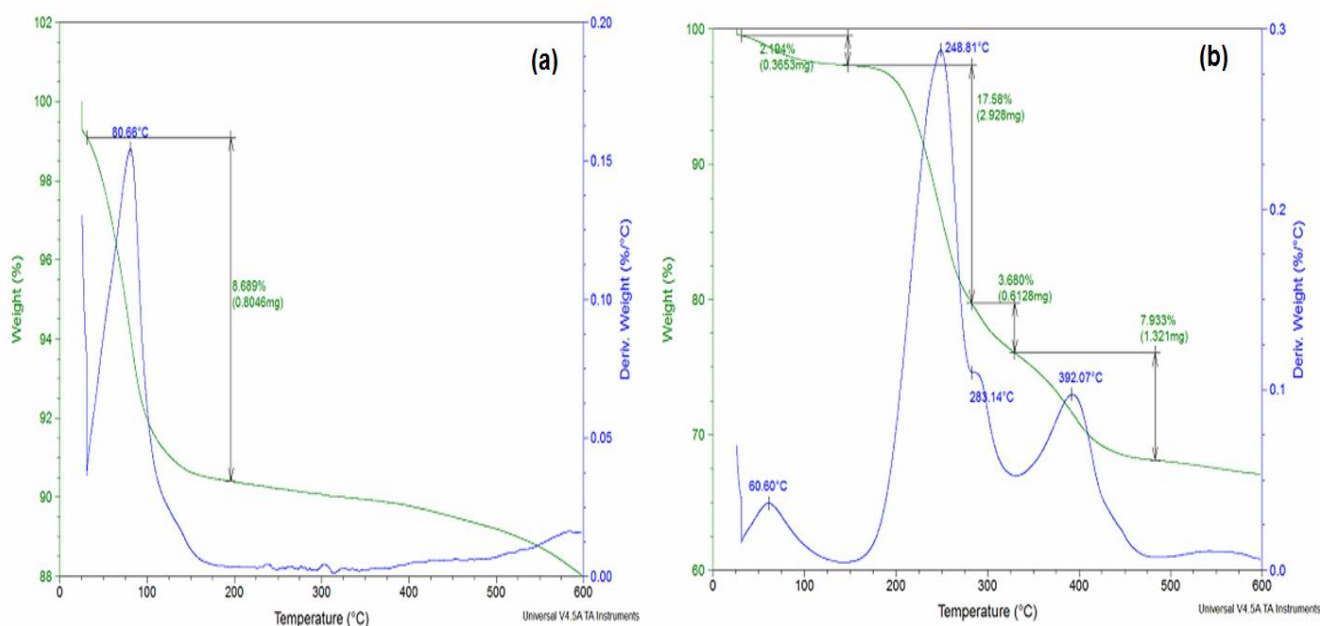


**Fig. 2.** TGA/DTG analysis of bentonite (a) and HDTMA-bentonite (b).

capacity.

## MATERIALS AND METHODS

### Preparation of Organo-clay

The natural bentonite utilized in this study was from Hammam Bouhrara deposit. The deposit is located in the

region of Maghnia (west of Algeria). Chemical composition of this clay was published in the literature as follows : 69.4% SiO<sub>2</sub>, 14.7% Al<sub>2</sub>O<sub>3</sub>, 1.2% Fe<sub>2</sub>O<sub>3</sub>, 1.1% MgO, 0.8% K<sub>2</sub>O, 0.5% Na<sub>2</sub>O, 0.3% CaO, 0.2% TiO<sub>2</sub>, 0.05% and 11% loss of ignition [11]. The cation exchange capacity (CEC) was found to be 97 meq g/100 g [12].

The sodium exchanged form of the bentonite (Na-

bentonite) was prepared from natural bentonite according to the procedure described in our previous work [13]. In order to enhance adsorption capacity of natural bentonite, Na-bentonite was modified with cationic surfactant hexadecyltrimethylammonium bromide (HDTMA), the modification was obtained by a cationic ion exchange reaction between  $\text{Na}^+$  and  $\text{HDTMA}^+$  [14]. For this purpose, 20 g of Na-bentonite was stirred magnetically for 48 h at room temperature ( $20 \pm 2$  °C) with 200 ml of HDTMA aqueous solution [15]. The amount of HDTMA is taken equal 100% the CEC of natural bentonite. After filtration, the organically obtained material was washed several times with deionized water until no bromide ion was detected with 0.1 M  $\text{AgNO}_3$  test [16,17].

### Preparation of Adsorbate

The HA stock solution ( $100 \text{ mg l}^{-1}$ ) was prepared by dissolving 100 mg of HA in 20 ml NaOH (0.025 M) and completing at 1 l with deionized water. The experimental solutions were prepared by diluting stock solution to the desired initial concentrations ( $C_0$ ).

### Characterization of Modified Clay

Natural bentonite and HDTMA-bentonite clays were analyzed using thermal analysis (TGA), infra-red analysis (FTIR) and X-ray diffraction. Thermal decomposition of bentonite samples was performed using a TA Instruments TGA 2050 Thermogravimetric Analyzer. The characteristic feature of this equipment was that the heating rate was coupled with the mass loss. Therefore, the temperature of the sample was kept constant until the mass loss corresponding to a chemical reaction was completed. The thermal evolution of the natural materials was followed from room temperature up to 600 °C. The average mass of the sample used was of about 20 mg. Chemical modification of clay was confirmed by FTIR spectra obtained by a spectrophotometer (Spectrum One FTIR spectrometer of Perkin Elmer) in the wave number range of  $4000\text{-}650 \text{ cm}^{-1}$ .

The internal structural modifications of bentonite clay were studied by X-ray powder diffraction technique using a Bruker D8 advance diffractometer, equipped with a  $\text{Cu K}\alpha$  source of radiation and a fast detector Lynxeyes (system  $\theta\text{-}\theta$ ) and working at the monochromatic radiation  $\text{K}\alpha_1$  wavelength of copper ( $\lambda = 1.5406 \text{ \AA}$ ). The radial scans

were measured in the reflection mode from  $2\theta = 8$  to  $80^\circ$ .

## RESULTS AND DISCUSSION

### Thermogravimetric Analyses

The TGA and derivative thermogravimetric (DTG) curves of natural bentonite and HDTMA-bentonite are illustrated in Figs. 2a and 2b, respectively. The TGA/DTG curves of the natural bentonite are shown in Fig. 2a. These curves show a single stage of mass loss at the mean temperature of 80.7 °C (8.7% of mass loss) associated the desorption of physically adsorbed water. On the other hand, no mass loss of bentonite is observed in the temperature range of 150-500 °C which means that the clay is relatively stable in this range of temperature.

The TGA/DTG curves of HDTMA-bentonite are given in Fig. 2b. TGA curve showed three stages of the mass loss. In the first stage, at the mean temperature of 60.6 °C (2.2% of mass loss), clay dehydration occurs. This mass loss is lower for HDTMA-bentonite than that for natural bentonite which confirms the hydrophobic nature of the modified bentonite [18]. The second stage occurs in the temperature range of 200-325 °C, DTG curve showed an intense peak at 248.8 °C (17.6% of mass loss). Knowing that pure HDTMA is decomposed at the same temperature, this peak corresponds to the decomposition of the surfactant on the surface of bentonite [16]. The third stage occurs in the temperature range of 325-450 °C (7.9% of mass loss) indicating the surfactant decomposition in the interlayer spaces of the bentonite clay [16,18].

### FT-IR Analysis

The FTIR spectra of bentonite and HDTMA-bentonite are illustrated in Fig. 3. Regarding Fig. 3 for both bentonite (a) and HDTMA-bentonite (b), the peak at 3615 is assigned to H-O-H stretching vibration bands of water molecules attached to weakly hydrogen bonded to the Si-O surface [16]. The broad band at  $3390 \text{ cm}^{-1}$  is due to H-O-H vibration of adsorbed water [19]. Furthermore, the peak around  $1635 \text{ cm}^{-1}$  corresponds to the OH deformation of water. The adsorbed water band's intensities are lower in the case of HDTMA-bentonite. This result confirms once again the hydrophobic nature of the modified bentonite, which is in good agreement with TGA results and with the literature

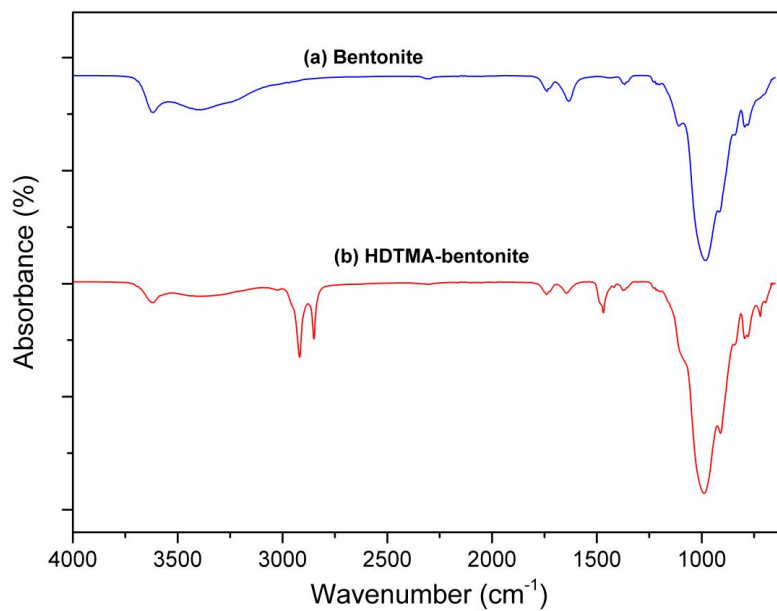


Fig. 3. FTIR spectra of bentonite (a) and HDTMA-bentonite (b).

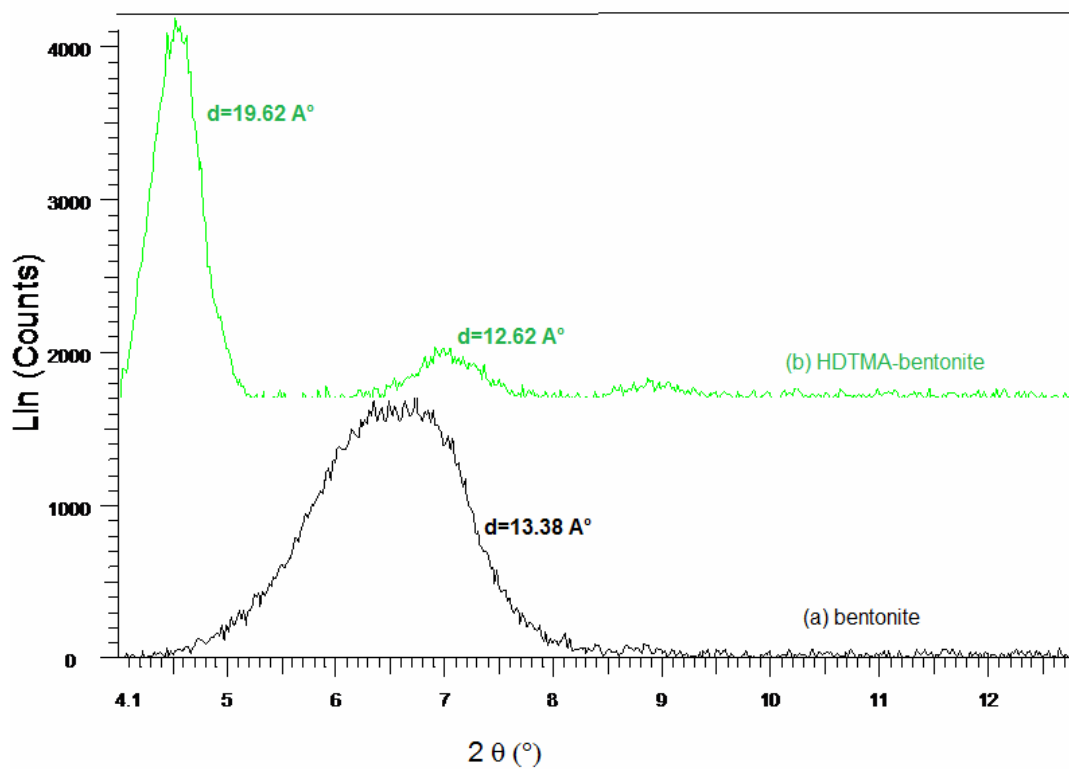


Fig. 4. XRD patterns of bentonite (a) and HDTMA-bentonite (b).

[16,18].

The two intensive peaks at 2850 and 2920  $\text{cm}^{-1}$ , corresponding to the anti-symmetric and symmetric  $\text{CH}_2$  stretching vibrations [20] and their bending vibrations at 1468 and 1418  $\text{cm}^{-1}$ , were only observed on HDTMA-bentonite (Fig. 3b). The presence of HDTMA is also confirmed by the significant peak at 720  $\text{cm}^{-1}$  (Fig. 3b) corresponding to the  $\text{CH}_2$  rocking band.

The intercalation of HDTMA surfactant results in the shift of the band of Al-OH-Al from 916 to 910  $\text{cm}^{-1}$ . At the same time, the most intensive band of Si-O-Si stretching moves from 982 to 988  $\text{cm}^{-1}$ .

### XRD Analysis

The XRD patterns of bentonite (a) and HDTMA-bentonite (b) are illustrated in Fig. 4. The  $d_{001}$  reflection peak occurs at  $2\theta = 6.6^\circ$  for bentonite (Fig. 4a) and shifts to smaller angle  $2\theta = 4.5^\circ$  for HDTMA-bentonite with a shoulder at  $2\theta = 7^\circ$  (Fig. 4b). This indicates the modification of the interlayer space of the bentonite clay by the intercalation of HDTMA molecule. In the case of bentonite, the interlayer distance observed was 13.38 Å (1.34 nm). For HDTMA-bentonite, the interlayer distance was increased to 19.62 Å (1.96 nm), similar results have been observed for Na-bentonite modified with 100% CEC equivalent concentration of HDTMA [18,21,22]. According to the literature, the length of the HDTMA<sup>+</sup> cation is 2.53 nm with 0.43 nm "nail-head" and 2.1 nm "nail-body". The height of the "nail-body" is between 0.41 and 0.46 nm and that of the "nail-head" is between 0.51 and 0.67 nm depending on whether a zigzag arrangement of the carbon atoms of HDTMA<sup>+</sup> is parallel to the plane of the bentonite layer, or perpendicular [21]. Knowing that the thickness of a single bentonite layer is about 0.96 nm [23,24], then the basal spacing of 1.96 nm of HDTMA-bentonite indicates a dimension of the interlayer space around 1 nm. This dimension of interlayer space indicated that HDTMA cations could have pseudotri-molecular arrangements in the interlayer space [23].

### Effect of Contact Time

Kinetic experiments were carried out at room temperature ( $20 \pm 2^\circ\text{C}$ ) in Erlenmeyer flasks containing HA aqueous solution at the initial concentration of 20  $\text{mg l}^{-1}$ . A

40 mg of bentonite or HDTMA-bentonite was added to 100 ml of HA solution and agitated magnetically at 300 rpm. Samples of 2 ml were withdrawn at suitable time intervals and centrifuged to remove the clay dispersion, and the HA residual concentration from the supernatant solution was measured by a UV-Vis spectrophotometer. The residual concentration of HA at time  $t$  ( $C_t$ ) allowed to calculate the quantity  $q_t$  ( $\text{mg g}^{-1}$ ) of the HA adsorbed by one gram of each adsorbent,

$$q_t = (C_0 - C_t) \frac{V}{m} \quad (1)$$

where  $q_t$  ( $\text{mg g}^{-1}$ ) is the adsorption capacity of bentonite or HDTMA-bentonite, and  $C_0$  ( $\text{mg l}^{-1}$ ) is the initial concentration of the adsorbate in the solution.  $V$  (l) is the volume of the HA solution, and  $m$  (g) is the mass of bentonite or HDTMA-bentonite used.

Figure 5 presents the variation of the adsorption capacity for HA onto bentonite and HDTMA-bentonite  $q_t$  ( $\text{mg g}^{-1}$ ) as a function of time  $t$  (min) at the initial concentration of 20  $\text{mg l}^{-1}$ . From this figure, it can be observed that the amount of HA adsorbed onto bentonite and HDTMA-bentonite was rapid initially and then slowed down gradually until they reached equilibrium around 120 min for bentonite and 210 min for HDTMA-bentonite. This is evident from the fact that in the beginning, a large number of vacant surface sites are available for HA, after a while the remaining vacant surface sites are hardly occupied due to repulsive forces between the HA molecules in the aqueous solution and those on the adsorbent surface [25-27].

As can be seen in Fig. 5, the adsorption capacity at equilibrium of HA onto HDTMA-bentonite (47.85  $\text{mg g}^{-1}$ ) is almost four times higher than the adsorption capacity of natural bentonite (11.23  $\text{mg g}^{-1}$ ). In reality and according to FTIR and TGA/DTG results, the surface of the modified HDTMA-bentonite is more hydrophobic than the surface of the natural bentonite. This increase in the hydrophobicity of HDTMA-bentonite enhances its adsorption capacity for organic pollutants, such as humic acid.

### Adsorption Kinetics

Kinetic studies of adsorption are helpful to understand

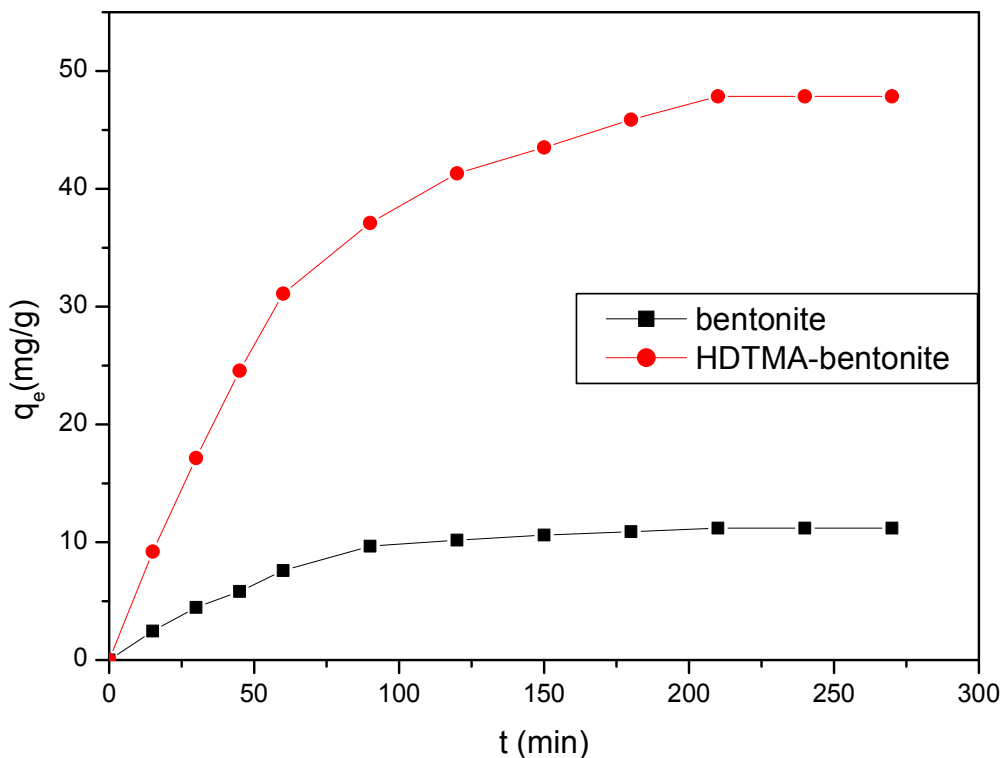


Fig. 5. Kinetics of the adsorption of HA on bentonite and HDTMA-bentonite.

Table 1. Pseudo-first-order PFO and Pseudo-second-order PSO Kinetic Parameters

Adsorbent	q <sub>e</sub> exp. (mg g <sup>-1</sup> )	Pseudo-first-order PFO			Pseudo-second-order PSO		
		K <sub>1</sub> (min <sup>-1</sup> )	q <sub>e</sub> cal. (mg g <sup>-1</sup> )	R <sup>2</sup>	K <sub>2</sub> (g mg <sup>1</sup> min <sup>-1</sup> )	q <sub>e</sub> cal. (mg g <sup>-1</sup> )	R <sup>2</sup>
Bentonite	11.2	0.020	12.18	0.99	9.61 10 <sup>-4</sup>	15.28	0.98
HDTMA-bentonite	47.8	0.01	50.69	0.99	1.78 10 <sup>-4</sup>	67.83	0.98

the mechanism of this process. Moreover, the knowledge of adsorption kinetics is crucial for designing adsorption processes. In the present study, the rates of adsorption of HA were determined with bentonite and HDTMA-bentonite.

In order to elucidate the adsorption mechanism of solid/liquid systems, two types of kinetics are generally

used, namely, the pseudo-first-order (PFO) and pseudo-second-order (PSO).

The PFO model [28,29] is expressed by the following equation:

$$\log(q_e - q_t) = \log(q_e) - \left(\frac{k_1}{2,303}\right)t \tag{2}$$

where  $q_e$  and  $q_t$  are the adsorption capacities of HA adsorbed onto the bentonite clays at equilibrium and after time  $t$ , respectively. The constant  $k_1$  ( $\text{min}^{-1}$ ) represent the PFO rate of adsorption. If the plot of  $\log(q_e - q_t)$  versus time is linear, then the value of  $k_1$  may be directly obtained from the slope of the plot.

The PSO model formula is generally employed in the form below [30]:

$$\frac{dq_t}{dt} = k_2(q_e - q_t)^2 \quad (3)$$

where  $k_2$  is the equilibrium rate constant of the PSO model ( $\text{g mg}^{-1} \text{min}^{-1}$ ).

The linear form of the previous equation is given as:

$$\frac{t}{q_t} = \frac{1}{k_2 \times q_e^2} + \frac{t}{q_e} \quad (4)$$

The slope and the intercept allow establishing  $q_e$  and  $k_2$ , respectively.

The PFO and PSO models were used to fit, by linear regression, the experimental data of HA adsorption onto bentonite and HDTMA-bentonite (figures not shown). The PFO and PSO rate constants  $k_1$  and  $k_2$  and the values of the theoretical  $q_e$  ( $q_e$  cal.) were calculated, and are given in Table 1. The values of the coefficient of determination  $R^2$  for both models are also calculated and grouped in Table 1. As can be seen from Table 1, the coefficient of determination  $R^2$  for PFO model was 0.99, higher than that for PSO model (0.98). The theoretical  $q_e$  ( $q_e$  cal.) obtained by PFO model is closer to the experimental data than the theoretical  $q_e$  values obtained by PSO model. This indicates the applicability of the PFO kinetic model to describe the adsorption process of HA onto both bentonite and HDTMA-bentonite.

### Adsorption Isotherms

Batch equilibrium experiments were carried out by contacting 40 mg of bentonite or HDTMA-bentonite with 100 ml of HA aqueous solution at different initial concentrations (2-50  $\text{mg l}^{-1}$ ) in 250 ml stopper Erlenmeyer. The solution was agitated magnetically at 300 rpm during 210 min.

The two classical models of Langmuir and Freundlich were tested to describe the adsorption equilibrium of HA onto both bentonite and HDTMA-bentonite.

The Langmuir equation can be written as follows [31]:

$$q_e = q_m \frac{K_L \times C_e}{1 + b.C_e} \quad (5)$$

where  $q_m$  ( $\text{mg g}^{-1}$ ) is the theoretical maximum monolayer adsorption capacity and  $K_L$  ( $\text{l mg}^{-1}$ ) is the Langmuir constant related to the energy of adsorption.

The dimensionless separation factor  $R_L$  gives an idea on the favorability of the adsorption process. In fact, according to  $R_L$  value, the shape of Langmuir isotherm is evaluated to be favorable ( $0 < R_L < 1$ ), unfavorable ( $R_L > 1$ ), irreversible ( $R_L = 0$ ) or linear adsorption ( $R_L = 1$ ) [30,32]. The smaller  $R_L$  value indicates a highly favorable adsorption.  $R_L$  values were calculated using the following equation:

$$R_L = \frac{1}{1 + K_L C_0} \quad (6)$$

The Freundlich model is expressed as follows [31]:

$$q_e = K_F C_e^{1/n} \quad (7)$$

where  $K_F$  and  $n$  are Freundlich constants, with  $K_F$  ( $\text{l g}^{-1}$ ) indicating the sorption capacity and  $n$  (dimensionless) indicating the favorable nature of the adsorption process. In reality, the Freundlich exponent ( $1/n$ ) explains the type of isotherm, when ( $1/n > 1$ ) the adsorption is unfavorable, ( $1/n = 1$ ) the adsorption is homogeneous and ( $0 < 1/n < 1$ ) the adsorption is favorable [33].

The plots of  $q_e$  versus  $C_e$  for the adsorption of HA onto bentonite and HDTMA-bentonite according to the non-linear form of Langmuir and Freundlich isotherm models were shown in Figs. 6a and 6b, respectively. All parameters were calculated by non-linear regression analysis of the corresponding isotherms and are given in Table 2.

For HA adsorption isotherms onto bentonite, it can be seen from Table 2 that the coefficient of determination  $R^2$  is high for both models, however with a better fit of the experimental data by means of Freundlich isotherm,

**Table 2.** Langmuir and Freundlich Isotherm Parameters

Adsorbent	Langmuir isotherm			Freundlich isotherm			
	$K_L$	$q_m$	$R^2$	$R_L$	$K_F$	$1/n$	$R^2$
Bentonite	0.019	54.80	0.838	0.92-0.31	2.26	0.64	0.889
HDTMA-bentonite	0.207	330.34	0.979	0.74-0.05	60.57	0.53	0.967

**Table 3.** Comparison of Maximum Monolayer Adsorption of HA onto Various Adsorbents

Adsorbent	$q_m$ ( $\text{mg g}^{-1}$ )	Ref.
Natural Algerian bentonite (Maghnia)	54.80	This work
Raw Jordanian bentonite (Azraq)	53	[34]
Acid-activated Greek bentonite	10.75	[35]
Activated carbon (Rice husk)	45.4	[36]
$\text{Fe}_3\text{O}_4$ -chitosan hybrid nano-particles	44.84	[37]
Zeolitic Imidazole Framework-8 (ZIF-8)	45	[38]
Modified HDTMA-bentonite	330.34	This work
HDTMA-bentonite	104.77	[39]
Amine-modified polyacrylamide-bentonite	174.03	[40]
ZnO-30N-zeolite	109-120	[41]

indicating the multilayer adsorption and the heterogeneity of the bentonite surface. In the case of HDTMA-bentonite, Langmuir model gives a better fit of the experimental data, proving monolayer and a homogenous surface of the HDTMA-bentonite adsorbent. The Langmuir maximum monolayer adsorption capacity  $q_m$  was found to be  $54.80 \text{ mg g}^{-1}$  and  $330.34 \text{ mg g}^{-1}$  for bentonite and HDTMA-bentonite, respectively. In addition, it can be seen that the values of  $R_L$  and  $1/n$  were found to be within the range of 0-1, indicating that the adsorption of HA onto both bentonite and HDTMA-bentonite is favorable according to Langmuir and Freundlich models. On the other hand, smallest values of  $R_L$  and  $1/n$  are obtained in the case of HA adsorption onto HDTMA-bentonite indicating that the adsorption is

more favorable in this case.

The comparison of maximum monolayer adsorption capacity  $q_m$  of HA onto various adsorbents is listed in Table 3, showing that  $q_m$  of natural Algerian bentonite used in the present work is comparable with some other reported adsorbents [34-38]. On the other hand, the modified HDTMA-bentonite prepared in this work showed a relatively large adsorption capacity of  $330.34 \text{ mg g}^{-1}$  compared to some adsorbents in previous literature studies [39-41].

### The Effect of pH on the HA Adsorption

The influence of pH on the adsorption of HA onto bentonite and HDTMA-bentonite was investigated in the pH

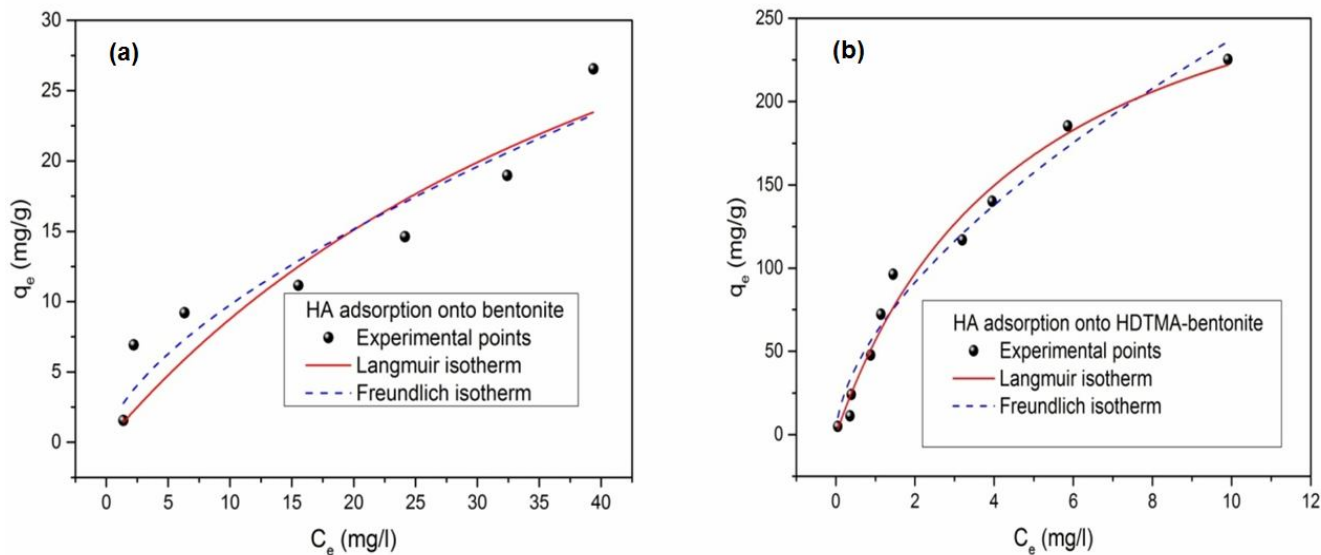


Fig. 6. Adsorption isotherms of HA onto bentonite (a) and HDTMA-bentonite (b).

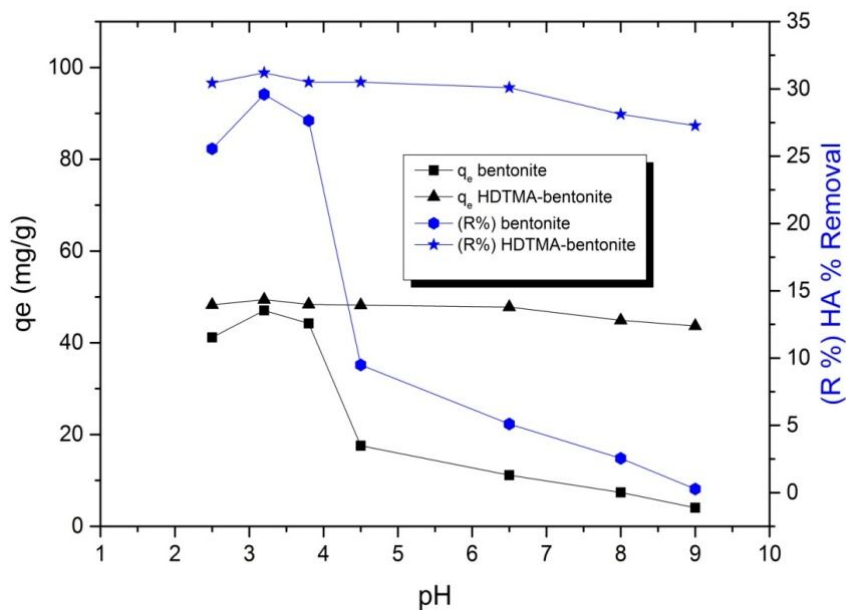
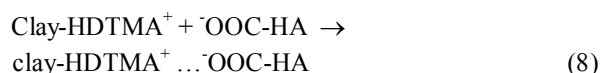


Fig. 7. Effect of pH on HA adsorption onto bentonite and HDTMA-bentonite.

range of 2.3-9. Figure 7 shows the variations in the removal of HA at various initial pHs. It was observed that the maximum quantity removed from HA was at pH 3.2 for both bentonite and HDTMA-bentonite. On the other hand, the adsorption capacity of bentonite decreases dramatically

from  $47.07 \text{ mg g}^{-1}$  to  $4.05 \text{ mg g}^{-1}$  with the increase of the pH of the solution from 2.3 to 9, similar results are reported in the literature [42]. The high adsorption of HA at lower pH values can be attributed to the external hydrogen bonds formed between phenolic hydroxyl groups of HA and the

hydrogen bonding sites on the clay [39]. In fact, the molecular form of HA dominating at low pH is hydrophobic and more absorbable than the ionized form as the hydrophobic bonding becomes the driving force for adsorption. Additionally, when the HA molecules approach to organic cations on the clay surface, the interaction between the positive surface and HA molecule is thermodynamically favored, and this results in expulsion of an acidic hydrogen from a carboxylic acid group of HA molecule to generate a negatively charged HA as shown by equation 8 [39].



Also from Fig. 7, It seems that the percentage removal of HA by HDTMA-bentonite is less pH-dependent than that by natural bentonite. Perhaps this is because the modification of bentonite by HDTMA surfactant resulted in a shift of the value of the surface charge of the clay from the acidic domain (for natural bentonite) to the basic domain for (HDTMA-bentonite) [43]. According to literature, the zeta-potential, which is directly related to the surface charge of the clay changed from negative value (for natural bentonite) to positive value for modified bentonite with HDTMA concentration higher than 93% CEC (in our case HDTMA concentration is equal to 100% CEC) [43]. Similar results are also reported in the case of zeolite modification by HDTMA [44].

## CONCLUSIONS

In this work, adsorption removal of humic acid from water using Algerian bentonite modified by intercalation with HDTMA was investigated. The results of characterization confirmed the modification of HDTMA-bentonite. Higher adsorption capacity and removal efficiency values were obtained with modified HDTMA-bentonite. The quantity of adsorbed humic acid ranged from 11.2 mg g<sup>-1</sup> for bentonite to 47.85 mg g<sup>-1</sup> for HDTMA-bentonite, which means that the adsorption capacity of HDTMA-bentonite is four times greater than that of natural bentonite. Freundlich model describes well the HA adsorption onto bentonite, while Langmuir model was

adequate for HA adsorption onto HDTMA-bentonite. The theoretical monolayer adsorption capacity  $q_m$  was found to be 50.80 mg g<sup>-1</sup> and 330.34 mg g<sup>-1</sup> for bentonite and HDTMA-bentonite, respectively. The kinetic study indicated that the adsorption process obeyed the pseudo-first-order model for both adsorbents. The results of the present investigation show that natural and modified Algerian bentonites may be used as a low-cost, natural, and abundant source for the removal of humic acid from aqueous solutions.

## ACKNOWLEDGMENTS

The authors are grateful to the Algerian Ministry of Higher Education and Scientific Research for financial support.

## REFERENCES

- [1] Schmidt, M. W. I.; Torn, M. S.; Abiven, S.; Dittmar, T.; Guggenberger, G.; Janssens, I. A.; Kleber, M.; Kögel-Knabner, I.; Lehmann, J.; Manning, D. A. C.; Nannipieri, P.; Rasse, D. P.; Weiner, S.; Trumbore, S. E., Persistence of soil organic matter as an ecosystem property. *Nature* **2011**, *478*, 49-56, DOI: 10.1038/nature10386.
- [2] Stevenson, F. J., *Humus Chemistry: Genesis, Composition, Reactions*; John Wiley & Sons, 1994; ISBN 0-471-59474-1.
- [3] Sehaqui, H.; Larraya, U. P. de.; Tingaut, P.; Zimmermann, T., Humic acid adsorption onto cationic cellulose nanofibers for bioinspired removal of copper (ii) and a positively charged dye. *Soft Matter*. **2015**, *11*, 5294-5300, DOI: 10.1039/C5SM00566C.
- [4] Cui, X.; Choo, K. -H., Natural organic matter removal and fouling control in low-pressure membrane filtration for water treatment. *Environ. Eng. Res.* **2014**, *19*, 1-8, DOI: 2014.19.1.1.
- [5] Budd George, C.; Hess Alan, F.; Shorney Darby, H.; Neemann Jeff, J.; Spencer Catherine, M.; Bellamy Julia, D.; Hargette Paul, H., Coagulation applications for new treatment goals. *J. -Am. Water Works Assoc.* **2004**, *96*, 102-113, DOI: 10.1002/j.1551-8833.2004.tb10559.x.

- [6] Sillanpää, M.; Ncibi, M. C.; Matilainen, A., Advanced oxidation processes for the removal of natural organic matter from drinking water sources: A comprehensive review. *J. Environ. Manage.* **2018**, *208*, 56-76, DOI: 10.1016/j.jenvman.2017.12.009.
- [7] Iriarte-Velasco, U. I.; Álvarez-Uriarte, J.; Chimeno-Alanís, N. R.; González-Velasco, J., Natural organic matter adsorption onto granular activated carbons: Implications in the molecular weight and disinfection byproducts formation. *Ind. Eng. Chem. Res.* **2008**, *47*, 7868-7876, DOI: 10.1021/ie800912y.
- [8] Bhatnagar, A.; Sillanpää, M., Removal of natural organic matter (NOM) and its constituents from water by adsorption-A review. *Chemosphere* **2017**, *166*, 497-510, DOI: 10.1016/j.chemosphere.2016.09.098.
- [9] Pandey, S., A comprehensive review on recent developments in bentonite-based materials used as adsorbents for wastewater treatment. *J. Mol. Liq.* **2017**, *241*, 1091-1113, DOI: 10.1016/j.molliq.2017.06.115.
- [10] Mowafa, T., The Mineral Industry of Algeria; 2013 Minerals Yearbook; U.S. Geological Survey, U.S. Department of the Interior, 2015; p. 13;.
- [11] Zaghoulane-Boudiaf, H.; Boutahala, M.; Sahnoun, S.; Tiar, C.; Gomri, F., Adsorption characteristics, isotherm, kinetics, and diffusion of modified natural bentonite for removing the 2,4,5-trichlorophenol. *Appl. Clay Sci.* **2014**, *90*, 81-87, DOI: 10.1016/j.clay.2013.12.030.
- [12] Aliouane, N.; Hammouche, A.; De Doncker, R. W.; Telli, L.; Boutahala, M.; Brahimi, B., Investigation of hydration and protonic conductivity of H-montmorillonite. *Solid State Ion.* **2002**, *148*, 103-110, DOI: 10.1016/S0167-2738(02)00049-8.
- [13] Bougdah, N.; Messikh, N.; Bousba, S.; Magri, P.; Djazi, F.; Zaghdoudi, R., Adsorption of humic acid from aqueous solution on different modified bentonites. *Chem. Eng. Trans.* **2017**, 223-228, DOI: 10.3303/CET1760038.
- [14] Dammak, N.; Fakhfakh, N.; Fourmentin, S.; Benzina, M., Treatment of gas containing hydrophobic VOCs by adsorption process on raw and intercalated clays. *Res. Chem. Intermed.* **2015**, *41*, 5475-5493, DOI: 10.1007/s11164-014-1675-9.
- [15] Al-Asheh, S.; Banat, F.; Abu-Aitah, L., Adsorption of phenol using different types of activated bentonites. *Sep. Purif. Technol.* **2003**, *33*, 1-10, DOI: 10.1016/S1383-5866(02)00180-6.
- [16] Erdem, B.; Özcan, A. S.; Özcan, A., Preparation of HDTMA-bentonite: Characterization studies and its adsorption behavior toward dibenzofuran. *Surf. Interface Anal.* **2010**, *42*, 1351-1356, DOI: 10.1002/sia.3230.
- [17] Hu, Z.; He, G.; Liu, Y.; Dong, C.; Wu, X.; Zhao, W., Effects of surfactant concentration on alkyl chain arrangements in dry and swollen organic montmorillonite. *Appl. Clay Sci.* **2013**, *75-76*, 134-140, DOI: 10.1016/j.clay.2013.03.004.
- [18] Houhoune, F.; Nibou, D.; Chegrouche, S.; Menacer, S., Behaviour of modified hexadecyltrimethylammonium bromide bentonite toward uranium species. *J. Environ. Chem. Eng.* **2016**, *4*, 3459-3467, DOI: 10.1016/j.jece.2016.07.018.
- [19] Lewinsky, A. A., Hazardous Materials And Wastewater: Treatment, Removal And Analysis; 1 edition.; Nova Science Pub Inc: New York, 2006; ISBN 978-1-60021-257-4.
- [20] Wang, Y. -Q.; Zhang, Z.; Li, Q.; Liu, Y. -H., Adsorption of uranium from aqueous solution using HDTMA+pillared bentonite: isotherm, kinetic and thermodynamic aspects. *J. Radioanal. Nucl. Chem.* **2012**, *293*, 231-239, DOI: 10.1007/s10967-012-1659-4.
- [21] Kaluderović, L. M.; Tomić, Z. P.; Đurović-Pejčev, R. D.; Vulić, P. J.; Ašanin, D. P., Influence of the organic complex concentration on adsorption of herbicide in organic modified montmorillonite. *J. Environ. Sci. Health Part B* **2017**, *52*, 291-297, DOI: 10.1080/03601234.2017.1281636.
- [22] Jović-Jovičić, N.; Milutinović-Nikolić, A.; Banković, P.; Dojčinović, B.; Nedić, B.; Gržetić, I.; Jovanović, D., Synthesis, characterization and adsorptive properties of organobentonites. *ACTA Phys. Pol. A* **2010**, *117*, 849-854.
- [23] Zhu, J.; He, H.; Guo, J.; Yang, D.; Xie, X., Arrangement models of alkylammonium cations in the interlayer of HDTMA+pillared montmorillonites. *Chin. Sci. Bull.* **2003**, *48*, 368-372, DOI: 10.1007/

- BF03183232.
- [24] Zhu, L.; Ruan, X.; Chen, B.; Zhu, R., Efficient removal and mechanisms of water soluble aromatic contaminants by a reduced-charge bentonite modified with benzyltrimethylammonium cation. *Chemosphere* **2008**, *70*, 1987-1994, DOI: 10.1016/j.chemosphere.2007.09.042.
- [25] Lin, J.; Zhan, Y., Adsorption of humic acid from aqueous solution onto unmodified and surfactant-modified chitosan/zeolite composites. *Chem. Eng. J.* **2012**, *200-202*, 202-213, DOI: 10.1016/j.cej.2012.06.039.
- [26] Uslu, H., Adsorption equilibria of formic acid by weakly basic adsorbent Amberlite IRA-67: Equilibrium, kinetics, thermodynamic. *Chem. Eng. J.* **2009**, *155*, 320-325, DOI: 10.1016/j.cej.2009.06.040.
- [27] Suresh, S.; Sundaramoorthy, S. Green Chemical Engineering: An Introduction to Catalysis, Kinetics, and Chemical Processes; CRC Press, 2014, ISBN 978-1-4665-5885-4.
- [28] Zhu, L.; Chen, B.; Shen, X., Sorption of phenol, p-nitrophenol, and aniline to dual-cation organobentonites from water. *Environ. Sci. Technol.* **2000**, *34*, 468-475, DOI: 10.1021/es990177x.
- [29] Dawood, S.; Sen, T. K., Removal of anionic dye Congo red from aqueous solution by raw pine and acid-treated pine cone powder as adsorbent: equilibrium, thermodynamic, kinetics, mechanism and process design. *Water Res.* **2012**, *46*, 1933-1946, DOI: 10.1016/j.watres.2012.01.009.
- [30] Bousba, S.; Meniai, A. Hassen, Adsorption of 2-chlorophenol onto sewage sludge based adsorbent: equilibrium and kinetic study. *Chem. Eng. Trans.* **2013**, 859-864, DOI: 10.3303/CET1335143.
- [31] Bousba, S.; Meniai, A. H., Removal of phenol from water by adsorption onto sewage sludge based adsorbent. *Chem. Eng. Trans.* **2014**, 235-240, DOI: 10.3303/CET1440040.
- [32] Babaei, A. A.; Khataee, A.; Ahmadpour, E.; Sheydaei, M.; Kakavandi, B.; Alaee, Z., Optimization of cationic dye adsorption on activated spent tea: Equilibrium, kinetics, thermodynamic and artificial neural network modeling. *Korean J. Chem. Eng.* **2016**, *33*, 1352-1361, DOI: 10.1007/s11814-014-0334-6.
- [33] Kim, D.; Ryoo, K. S., A study on adsorption of Li from aqueous solution using various adsorbents. *Bull. Korean Chem. Soc.* **2015**, *36*, 1089-1095, DOI: 10.1002/bkcs.10200.
- [34] Salman, M.; El-Eswed, B.; Khalili, F., Adsorption of humic acid on bentonite. *Appl. Clay Sci.* **2007**, *38*, 51-56, DOI: 10.1016/j.clay.2007.02.011.
- [35] Doulia, D.; Leodopoulos, C.; Gimouhopoulos, K.; Rigas, F., Adsorption of humic acid on acid-activated Greek bentonite. *J. Colloid Interface Sci.* **2009**, *340*, 131-141, DOI: 10.1016/j.jcis.2009.07.028.
- [36] Daifullah, A. A. M.; Girgis, B. S.; Gad, H. M. H., A study of the factors affecting the removal of humic acid by activated carbon prepared from biomass material. *Colloids Surf. Physicochem. Eng. Asp.* **2004**, *235*, 1-10, DOI: 10.1016/j.colsurfa.2003.12.020.
- [37] Zulfikar, M. A.; Afrita, S.; Wahyuningrum, D.; Ledyastuti, M. Preparation of Fe<sub>3</sub>O<sub>4</sub>-chitosan hybrid nano-particles used for humic acid adsorption. *Environ. Nanotechnol. Monit. Manag.* **2016**, *6*, 64-75, DOI: 10.1016/j.enmm.2016.06.001.
- [38] Lin, K. -Y. A.; Chang, H. -A., Efficient adsorptive removal of humic acid from water using zeolitic imidazole framework-8 (ZIF-8). *water. Air. Soil Pollut.* **2015**, *226*, 10, DOI: 10.1007/s11270-014-2280-7.
- [39] Anirudhan, T.; Ramachandran, M., Surfactant-modified bentonite as adsorbent for the removal of humic acid from wastewaters. *Appl. Clay Sci.* **2007**, *35*, 276-281, DOI: 10.1016/j.clay.2006.09.009.
- [40] Anirudhan, T. S.; Suchithra, P. S.; Rijith, S., Amine-modified polyacrylamide-bentonite composite for the adsorption of humic acid in aqueous solutions. *Colloids Surf. Physicochem. Eng. Asp.* **2008**, *326*, 147-156, DOI: 10.1016/j.colsurfa.2008.05.022.
- [41] Wang, L.; Han, C.; Nadagouda, M. N.; Dionysiou, D. D., An innovative zinc oxide-coated zeolite adsorbent for removal of humic acid. *J. Hazard. Mater.* **2016**, *313*, 283-290, DOI: 10.1016/j.jhazmat.2016.03.070.
- [42] Derakhshani, E.; Naghizadeh, A., Optimization of humic acid removal by adsorption onto bentonite and montmorillonite nanoparticles. *J. Mol. Liq.* **2018**, *259*, 76-81, DOI: 10.1016/j.molliq.2018.03.014.

- [43] Schampera, B.; Tunega, D.; Šolc, R.; Woche, S. K.; Mikutta, R.; Wirth, R.; Dultz, S.; Guggenberger, G., External surface structure of organoclays analyzed by transmission electron microscopy and X-ray photoelectron spectroscopy in combination with molecular dynamics simulations. *J. Colloid Interface Sci.* **2016**, *478*, 188-200, DOI: 10.1016/j.jcis.2016.06.008.
- [44] Li, C.; Dong, Y.; Wu, D.; Peng, L.; Kong, H., Surfactant modified zeolite as adsorbent for removal of humic acid from water. *Appl. Clay Sci.* **2011**, *52*, 353-357, DOI:10.1016/j.clay.2011.03.015.